Supporting Information for:

Electrochemical sensing with single nanoskived gold nanowires bisecting a microchannel

Pieter E. Oomen,[†] Yanxi Zhang,[‡] Ryan C. Chiechi,[‡] Elisabeth Verpoorte,[†] and Klaus Mathwig[,†]*

[†] University of Groningen, Groningen Research Institute of Pharmacy, Pharmaceutical Analysis, P.O. Box 196, 9700 AD Groningen, The Netherlands

[‡] Stratingh Institute for Chemistry, University of Groningen, Nijenborgh 4, 9747 AG Groningen, The Netherlands

Contents

1. Experimental details

1.1 Nanoskiving

Gold nanowires were prepared by nanoskiving as described previously [1]. In brief, 200-nm-thick Au films were deposited onto silicon wafers through a Teflon mask by thermal evaporation. The thickness of the Au film controlled the height of the nanowire, whereas the lateral dimension of the film controlled the length of the nanowires. Epofix epoxy resin (Electron Microscope Sciences, USA) was used to cover the gold film and silicon wafer. After curing, the epoxy containing the gold films was lifted from the wafer using a razor blade. The epoxy around the films was cut out into blocks to fit into molds used for embedding samples for standard ultramicrotomy. The mold with epoxy blocks was filled with more epoxy and cured at 60 °C to completely embed the gold film. Using an ultramicrotome (Leica UC-6, The Netherlands), 200-nm-thick sections were skived from the block and floated onto a water bath. Each section contained a single nanowire surrounded by epoxy. The thickness of the sections dictates the width of the nanowires. Using a small loop tool, sections were transported *via* a droplet of water. The wires produced in this fashion were 200 nm x 200 nm x 1.5 mm.

1.2 Microfluidic device fabrication

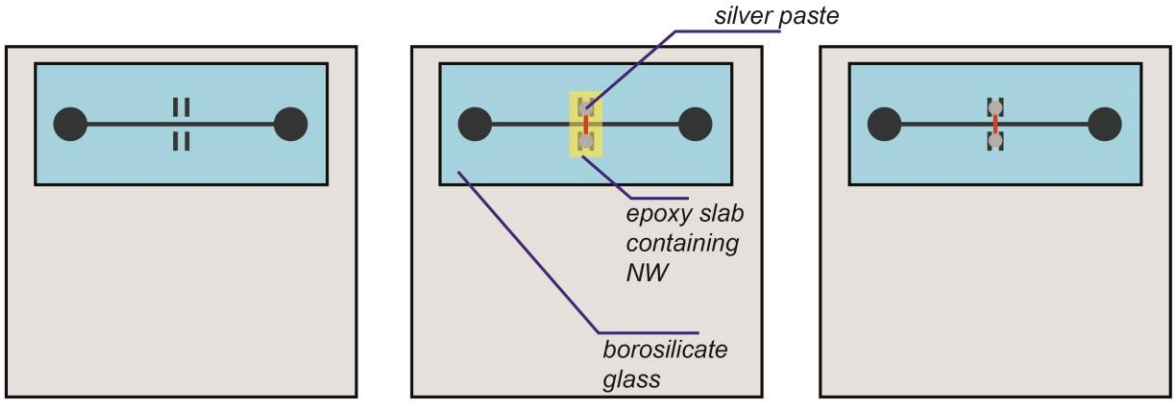

1. A borosolicate substrate with microchannels is glued to a square microscopy slide.

2. Using a droplet of water on a loop tool, a nanoskived epoxy section containing one gold nanowire is transferred to the substrate (alignment is facilitated by the etched marks perpendicular to the channel). After the water is evaporated, small drops of silver paste are applied to be able to electrically check the integrity of the wire using a multimeter.

3. If the wire is intact, the epoxy is etched away by exposing to oxygen plasma for 1 hour.

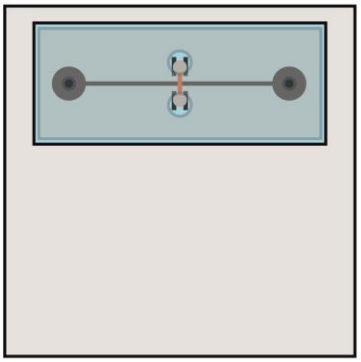

4. After a brief exposure to oxygen plasma, a complementary PDMS part with microchannels is covalently bonded to the glass substrates. For this, a custom-built aligner was used. The PDMS part contains small holes that allow acces to the now sealed microchannel, and to the conductive paste on the nanowire.

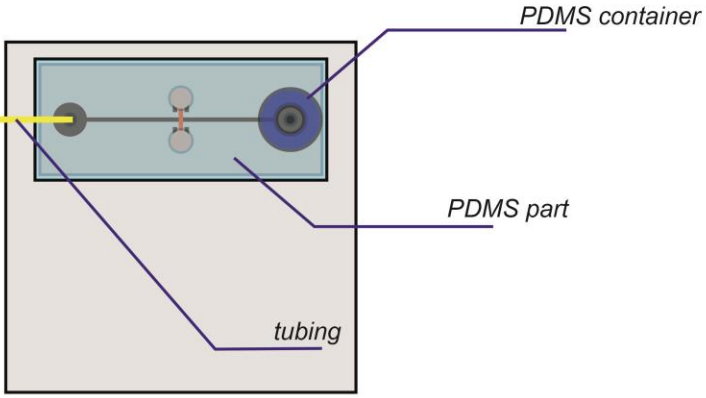

5. The holes over the nanowire are filled with additional silver paste to allow connection of the nanowire to analytical instruments. Tubing can be inserted at the inlet. A small PDMS container is glued to the outlet, where a reference electrode can be placed.

Figure S1: Top view schematic of the microfluidic device fabrication and nanowire integration. Dimensions not to scale.

The glass-PDMS devices used for the experiments with suspended gold nanowires bisecting a microfluidic channel were designed and fabricated in a manner similar to that described previously [1]. Figure S1 gives a schematic overview of the different steps involved in the process. In brief, 1-cm-long, 70-µm-wide and 30-µm-deep microchannels were patterned and then wet-etched in borosilicate (Schott Borofloat) wafers precoated with chromium and photoresist (Telic, USA) using HF-etching solution (1:1 mixture of 49% HF and 19.6% HNO_3, HF and HNO_3 from Merck, Germany). Using a sandblaster, rectangular substrates (1 x 2 cm) were cut out of the wafer, with each substrate featuring one microchannel. The substrates were glued to larger square microscopy slides for facile handling. Nanoskived epoxy sections containing gold nanowires were placed over the channels using a water droplet, making use of etched alignment marks in the glass for facile positioning. After the water was evaporated, small drops of conductive silver paste (Agar Scientific, UK) were added to check the wire integrity (conductivity) using a multimeter. The glass substrates were subsequently exposed to oxygen plasma for 1 h at 100 mTorr at 30 W in a plasma cleaner (Harrick Plasma, USA) to etch away the epoxy surrounding the gold nanowire. Complementary rectangular channels in PDMS (Sylgard, Dow Corning, USA) were made by casting uncured PDMS to glass wafers, patterned with SU-8 50 (Microchem, Germany) using soft lithography. Stainless steel pins (Ø 300 µm) were inserted through a 3D-printed template and aligned with the ends of the channel being molded to provide fluid inlets and outlets when the PDMS was cast. After curing, rectangular parts (1 cm x 2 cm), each containing one 1-cm-long, 80-µm-wide, 40-µm-deep microchannel, were cut out and lifted from the molds, and the stainless-steel pins were removed. Using a 3-mm-diameter biopsy punch (Kai Medical, Germany), holes were made next to the channel to align with the conductive paste applied to the nanowires on the glass substrates. After exposure to oxygen plasma for 1 minute, the glass substrate and PDMS were irreversibly bonded using the custom-built aligner described earlier.[1] This sealed the microchannels, leaving the nanowire suspended in the microchannel. Additional conductive paste was added through the punched holes in the PDMS to facilitate connection of the contact wire to analytical instruments (*i.e.*, a potentiostat).

A similar device was fabricated to monitor the electrochemical response of nanowires placed on the bottom of microchannels, but in this case skived sections were placed on flat glass substrates. After the epoxy was etched away using oxygen plasma, the wire was covered with an identical PDMS channel as used in the devices with suspended wires.

As stated in the main text, care should be taken when filling the channels with solution. Exposure to high flow rates before wetting or air bubbles may lead to breaking of the integrated nanowire because of the high surface tension at the liquid-air meniscus. Overall, the fabrication procedure is reproducible, but requires training and careful handling of the devices. We achieved a yield of 5-10% working devices at the end of the procedure. However, various control steps ensure that it is not necessary to complete the whole procedure before a faulty device is discovered. Furthermore, the glass substrates can be reused after careful cleaning and removal of PDMS residues.

1.3 Electrochemical measurements

A 1 mM solution of electroactive species ferrocene (VWR, The Netherlands) was prepared in acetonitrile (Biosolve B.V., The Netherlands) with 0.1 M tetrabutylammonium hexafluorophosphate ($TBAPF_6$, Sigma-Aldrich, The Netherlands) as supporting electrolyte. The solution was introduced into the channel from a 500 µL glass syringe through fluorinated ethylene propylene tubing (794 µm OD, 178 µm ID). The flow rate was controlled using a syringe pump (Harvard Apparatus, USA) initially set to 1 µL/min. At the outlet, the solution was collected in a small PDMS container, into which a Ag/Ag^+ reference electrode (BASi, USA) was submerged. The reference electrode was prepared by immersing a silver wire in a Luggin capillary (with Vicor tip) containing acetonitrile with 0.1 M $TBAPF_6$ and 0.01 M $AgNO_3$. CVs were recorded at a scan rate of 20 mV/s and different flow rates using a LabVIEW-controlled FEMTO DDPCA-300 transimpedance amplifier as potentiostat. The nanowire was in all cases interfaced through the connection pads in the punched holes of the PDMS part of the microfluidic device. The experiments under flow were conducted both on suspended nanowires and nanowires placed on flat glass substrates. Chronoamperometry (Figure 2B of the main text) was performed at a constant potential of 0.6 V *vs.* Ag/Ag^+.

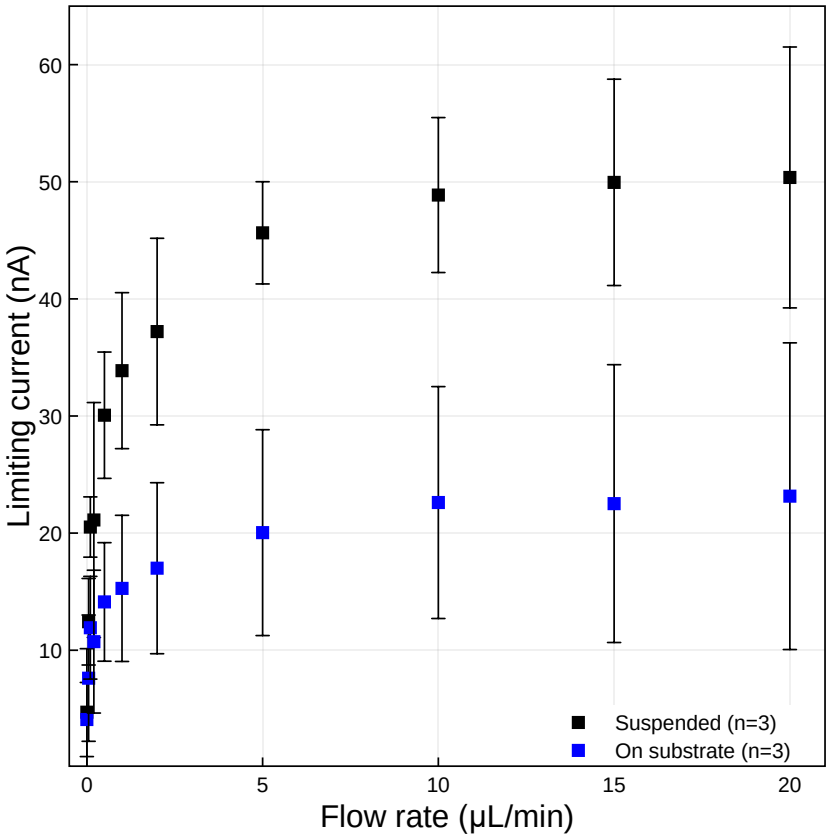

Figure S2: The limiting current generated at 0.6 V *vs*. Ag/Ag^+ by 1 mM ferrocene dissolved in acetonitrile containing 0.1 M $TBAPF_6$ electrolyte. Nanowires suspended in or placed at the bottom of a microchannel acted as the electrode (average ± standard deviation; n = 3: 3 different NW electrodes).

2. Limiting currents – suspended nanowires vs. nanowires on substrate

The limiting current (measured at 0.6 V) is plotted *vs.* the flow rate in Figure S2. It can be seen that the limiting current increases sublinearly and monotonically with flow rate, as observed previously for measurements using conventional microelectrodes [2]. Furthermore, following from the observed limiting currents, the detected current generated by suspended nanowires is on average 2.0 ± 0.3 times higher compared to nanowires placed on the bottom of the channel. The variation in wires from one device to the next is quite large (both in the case of suspended NWs and wires placed on substrates). This is likely due to the positioning of the wires. Still embedded in epoxy, the wires are picked up using a drop of water on a loop, and are subsequently manually positioned on the glass part of the device. Although we aimed for a perpendicular orientation of the wire with respect to the channel, this proved hard to reproduce in practice (as can also be seen in the Table of Contents Figure). This alters the available reaction surface of the nanowire, along with minor influences from incomplete removal of the epoxy slab during dry etching or artifacts introduced to the channel geometry during the etching of the glass channels. However, the results show that suspended NWs generate higher currents than NWs placed on a flat substrate when used as electrochemical sensing elements in microfluidic channels. In fact, in the case of NWs placed on the bottom of the channel, the channel height is also smaller compared to the case of suspended wires as no channels are etched into the borosilicate and the PDMS channels have a height of 40 µm. Relatively speaking, this leads to a faster overall flow velocity at the same flow rate due to the smaller cross-section, making the difference in current response even more pronounced.

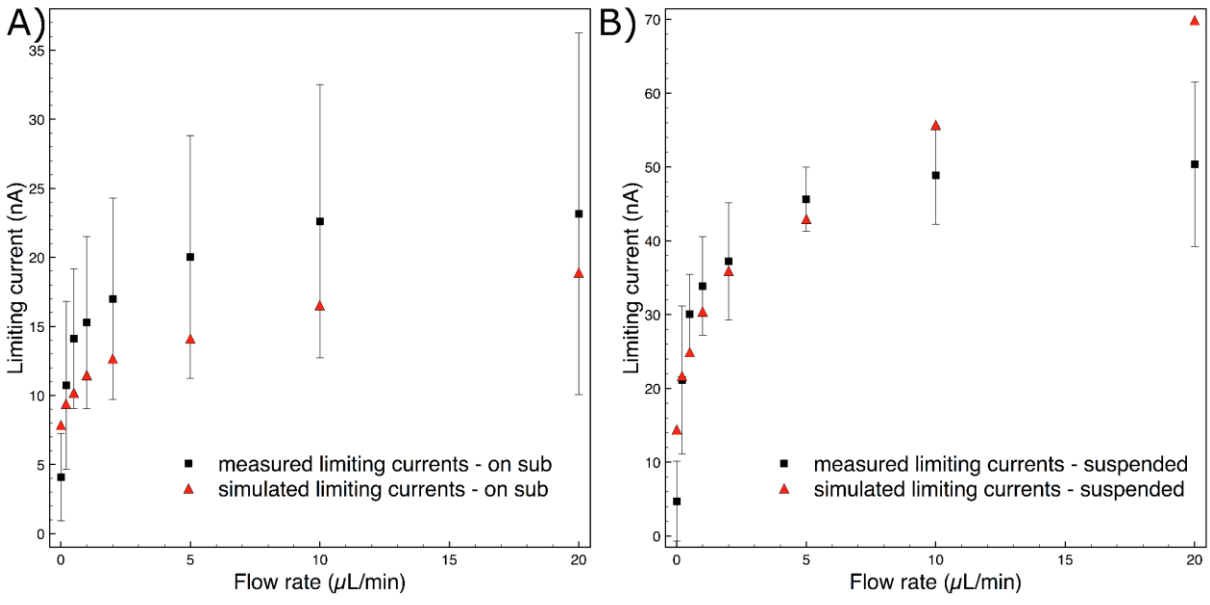

Figure S3: Limiting current generated at 0.6 V *vs.* Ag/Ag^+ by 1 mM ferrocene dissolved in acetonitrile containing 0.1 M $TBAPF_6$ electrolyte compared to theoretical limiting current based on simulated cyclic voltammograms (see main text). Nanowires placed at the bottom (A) or in the center (B) of a microchannel acted as the electrode (for experimental values: average ± standard deviation; *n* = 3: 3 different NW electrodes).

In Figure S3 a comparison between the limiting currents obtained from experimental and simulated cyclic voltammograms is provided for nanowires placed on substrates (left) and suspended (right) in microchannels. There is good agreement between the simulations and experiments.

Analytically, the relationship between limiting current in (quasi-)steady state and surface area of a nanochannel is best described and approximated by the 'band UME' [3] or 'nanoband' equation, which was previously employed successfully for Au NW electroanalysis (K. Dawson et al., *J. Phys. Chem. C* 2012 [4]):

$$i_L = \frac{2\pi FlDC}{\ln(\frac{64Dt}{w^2})}, \qquad \text{(S1)}$$

with i_L: limiting current; F: Faraday constant; l: wire length; D: diffusion coefficient (ferrocene in acetonitrile: $2.0 \cdot 10^{-9}$ m^2/s [5]); C: analyte concentration; t: time equal to RT/Fv, where R is the gas constant, T the temperature and v the scan rate; w: nanowire width. This nanoband equation yields the quasi-steady state limiting current for a recessed electrode with one side of a NW exposed to solution. For a 200 nm wide and 70 µm long electrode, a 20 mV/s scan rate and a 1 mM ferrocene concentration, the nanoband equation yields a current of 5.5 nA. This value compares well with the experimental values of the limiting current of suspended NWs of 4.7 ± 5.4 nA and NWs placed at the bottom of the microchannel of 4.1 ± 3.2 nA. Thus, within this uncertainty, a surface area of 200 nm by 70 µm is in good agreement with the theoretical expectation. The nanoband equation considers only a single nanowire surface as compared to three and four exposed surfaces in the experiment, respectively. Thus, eq. (S1) underestimates i_L.

A three-dimensional finite element simulation (COMSOL, see below) yields steady-state limiting currents which are higher but of the same order of magnitude: 14 nA for a suspended NW and 8 nA for a substrate NW. The table below compares all values:

	Experimental i_L	i_L nanoband eq. (S1)	i_L COMSOL
Suspended NW	4.7 ± 5.4 nA	5.5 nA	14 nA
NW at bottom	4.1 ± 3.2 nA		8 nA

We also note that there is additional uncertainty in the effective length of the NW. If it is placed at an angle of 25° compared to being perpendicular to the microchannel, the exposed length is increased by 10% to 70 µm/cos(25°) = 77 µm.

3. Simulations

A two-dimensional geometry of an 80-µm-long and 70-µm-high microchannel with a nanowire (square cross-section of 200 nm by 200 nm) was modeled and used for simulations in COMSOL Multiphysics. A flow velocity profile was determined by solving the Navier-Stokes equations for incompressible Stokes flow:

$$\nabla p = \eta \nabla^2 \boldsymbol{u}, \qquad \nabla \cdot \boldsymbol{u} = 0$$

The flow velocity profile $\boldsymbol{u}$ was evaluated for various inlet flow rates, a pressure of p=0 Pa at the microchannel outlet and no-slip boundaries at the microchannel walls and nanowire surfaces (η: dynamic viscosity of 0.334 mPa s [6]). Convective transport of a fully reduced analyte at a 1 mM concentration (initially in the bulk and constantly at the inlet and outlet boundaries) was modelled in the calculated Poiseuille flow profile, as well as by diffusion, by using the drift-diffusion equation (assuming a high electrolyte concentration and no migration):

$$\boldsymbol{u} \cdot \nabla c_{\mathrm{R,O}} = D \nabla^2 c_{\mathrm{R,O}}$$

Here, D is a diffusion coefficient of $2 \cdot 10^{-9}$ m^2/s [5] and $c_{\mathrm{R,O}}$ are the concentrations of reduced and oxidized species of initially 1 mM and 0 mM, respectively.

In Figure S4, simulated flow velocities in the channel around a suspended nanowire are shown for a flow rate of 20 µL/min. A gradient in flow velocities can be observed, ranging from about 0.1 m/s in the center of the channel (where suspended wires are situated), and approaching 0 m/s at the channel walls. This is in agreement with the lower current generated by nanowires placed on substrates, as experimentally assessed. The transport of analyte towards suspended nanowires is very fast due to the positioning in the flow profile. The disturbance of the flow profile caused by the nanowire itself is very small.

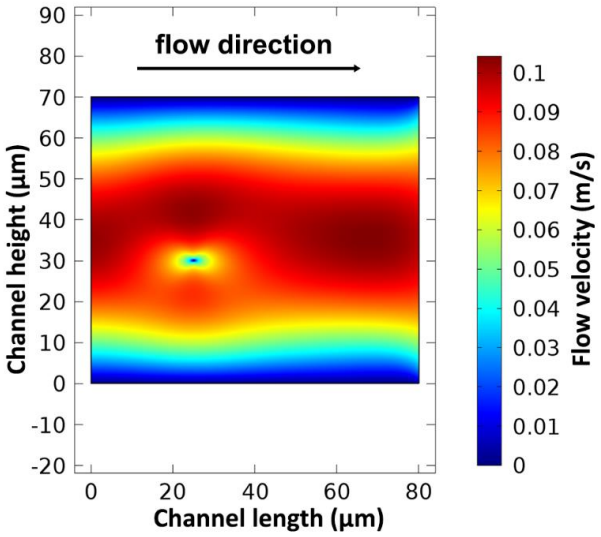

Figure S4: Cross-section of a segment of the microchannel with a suspended nanowire, showing the flow velocity profile around the nanowire.

In Figure S5, the concentration of oxidized product is shown in the channel at a flow rate of 20 µL/min, and at a potential of 0.6 V. This concentration profile shows that analyte transport is dominated by advection. This is further underlined by the approximate surface Péclet number for this system:

$$\mathrm{Pe} = \frac{Uh}{D}$$

Here, U is the average flow velocity in the channel (approximately 0.075 m/s) and h the height of the channel (70 µm). This equation gives an approximate surface Péclet number of 2625. Oxidized product molecules move along with the flow due to Stokes forces and a very steep concentration gradient is established at the side of the wire facing the flow inlet; diffusion of product from the wire through the rest of the channel is limited.

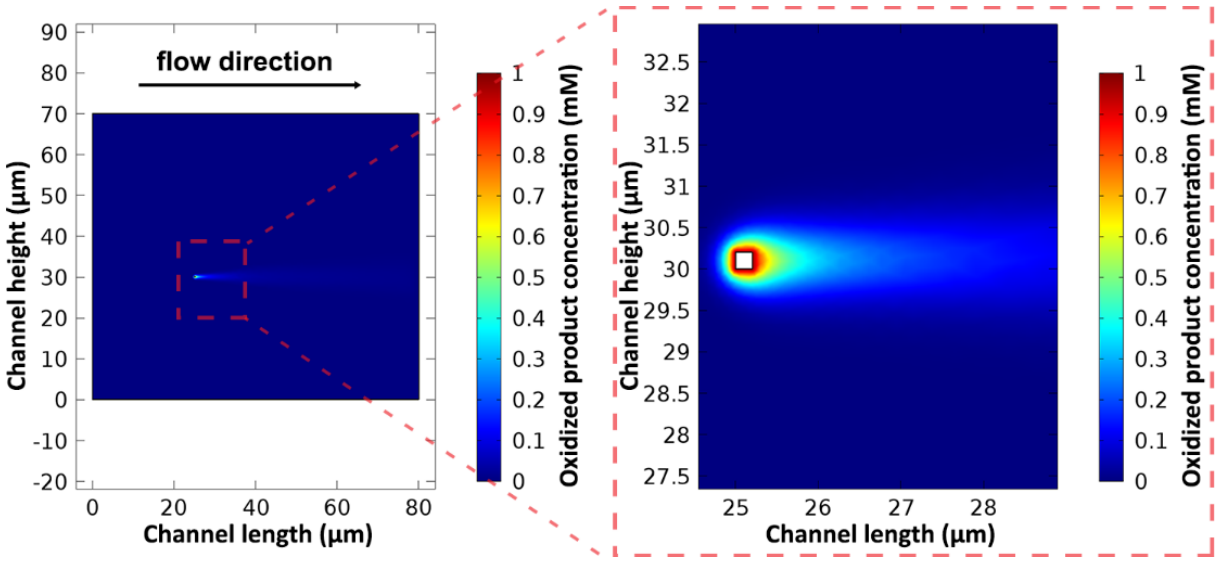

Figure S5: Cross-section of a segment of the microchannel with a suspended nanowire, showing the concentration of oxidized product around the nanowire (right: zoom).

In order to determine the formal potential E_h as well as the standard electrochemical rate constant k_0 (see Figure 3 in the main text), we fitted a Butler-Volmer equation [7] to experimental cyclic voltammograms:

$$i = \frac{i_{\mathrm{lim}}}{1+\exp\left[\frac{-F(E-E_h)}{RT}\right]+\frac{i_{\mathrm{lim}}}{AFCk_0}\exp\left[\frac{-F(1-\alpha)(E-E_h)}{RT}\right]}.$$

Here, the fitting parameters are the limiting current i_{lim} as well as E_h and k_0. A denotes the surface area of the nanowire electrode of 4 × 200 nm × 70 µm. The fit yields: E_h = 55 mV and k_0 = 0.5 cm/s.

4. Effect of nanowire diameter

To investigate the dependence of the nanowire size on the effect of the distortion of voltammograms, we numerically determined CVs of a suspended wire with a diameter ranging from 20 nm to 10 µm (quadratic cross section). The results are shown in Figure S6 for a fast flow rate of 20 µL/min and parameters otherwise identical to the simulations described above. The CVs are increasingly distorted towards higher potentials for decreasing wire size, and a symmetric CV shape is approached for a 10 µm thick wire. The limiting current increases sub-linearly with increasing wire diameter (see Fig. S6C).

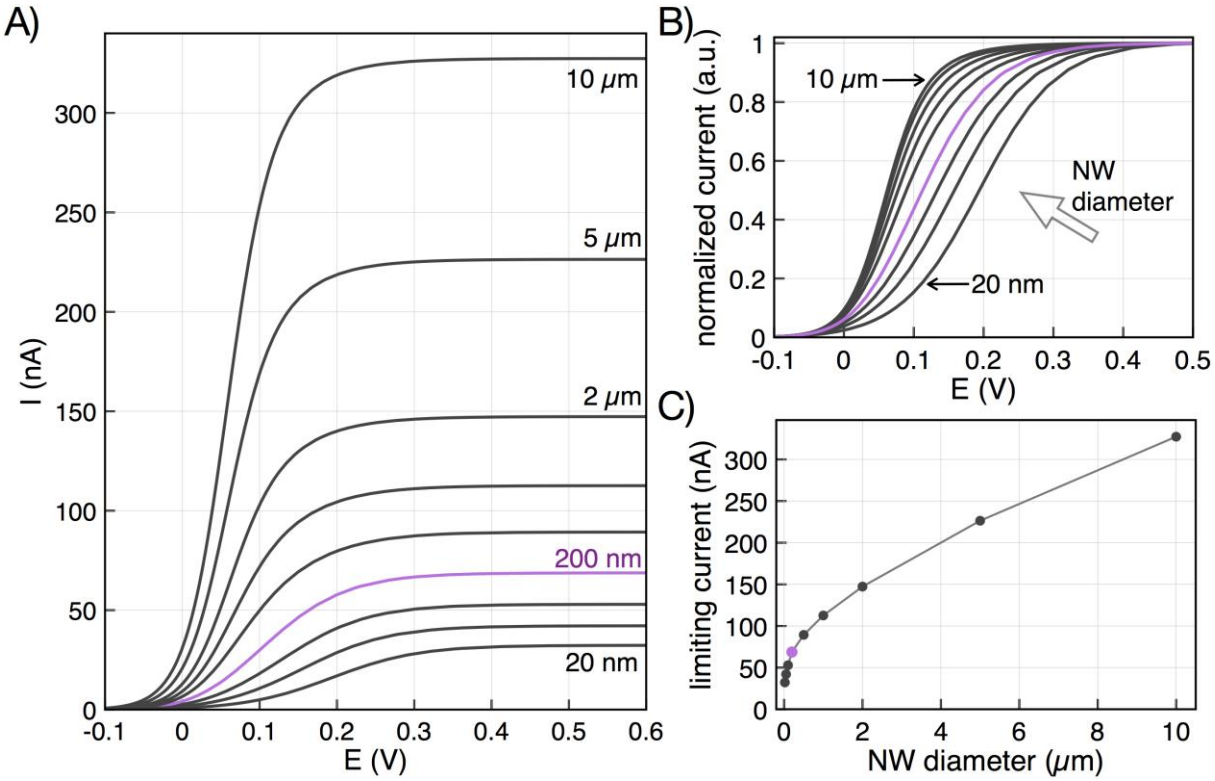

Figure S6: A) Numerical simulation of cyclic voltammograms as a function of the *diameter* of the nanowire bisecting a microchannel for a flow rate of 20 µL/min and nanowire diameters of 20 nm, 50 nm, 100 nm, 200 nm, 500 nm, 1000 nm, 2000 nm, 5000 nm, 10000 nm (quadratic cross section). The purple curve is identical to the 20-µL/min-curve in Fig. 2A in the main text. B) The same voltammograms normalized to a unity limiting current. C) Limiting current at 0.6 V as a function of the nanowire diameter.

References

1. Kalkman GA, Zhang Y, Monachino E, Mathwig K, Kamminga ME, Pourhossein P, Oomen PE, Stratmann SA, Zhao Z, van Oijen AM, et al. Bisecting Microfluidic Channels with Metallic Nanowires Fabricated by Nanoskiving. *ACS Nano* (2016) **10**:2852–2859.

2. Rassaei L, Mathwig K, Goluch ED, Lemay SG. Hydrodynamic Voltammetry with Nanogap Electrodes. *The Journal of Physical Chemistry C* (2012) **116**:10913–10916.

3. Bard AJ, Faulkner LR. *Electrochemical methods: fundamentals and applications*. Wiley New York (1980).

4. Dawson K, Wahl A, Murphy R, O'Riordan A. Electroanalysis at Single Gold Nanowire Electrodes. *J Phys Chem C* (2012) **116**:14665–14673. doi:10.1021/jp302967p

5. Tsierkezos NG. Cyclic Voltammetric Studies of Ferrocene in Nonaqueous Solvents in the Temperature Range from 248.15 to 298.15 K. *J Solution Chem* (2007) **36**:289–302.

6. Viscosity of Acetonitrile – viscosity table and viscosity chart. Available at: https://wiki.anton-paar.com/en/acetonitrile/ [Accessed July 30, 2018]

7. Dawson K, Strutwolf J, Rodgers KP, Herzog G, Arrigan DW, Quinn AJ, O'Riordan A. Single nanoskived nanowires for electrochemical applications. *Analytical chemistry* (2011) **83**:5535–5540.